Lowland Technology International 2018; 20 (3): 285-296
International Association of Lowland Technology (IALT): ISSN 1344-9656

Research Paper

Mechanical and hydrological time-dependent properties of granulated blast furnace slag-sand mixture in soft ground improvement

T. Sakata [1], N. Yasufuku [2], R.Ishikura [3] and A.Alowaisy [4]

ARTICLE INFORMATION

Article history:

Received: 21 July, 2018
Received in revised form: 21 September, 2018
Accepted: 25 September, 2018
Publish on: 07 December , 2018

Keywords:

Granulated blast furnace slag
Soil compaction piles
Hydration
Hydraulic conductivity
Mechanical characteristics

ABSTRACT

Every year about 20 million tons of Granulated Blast Furnace Slag (GBFS) are produced as a manufacturing byproduct. GBFS is mainly utilized in cement production accounting for 70% of the total utilized weight, while the geotechnical engineering applications accounts for 2%. Therefore, finding innovative utilization methods is a necessity. It was reported that the GBFS can be used as substitutive material in sand compaction pile (SCP) method. This study aims at evaluating the time-dependent mechanical, hydrological and chemical properties of the GBFS and the GBFS-sand mixtures. It was found that for early hydration stage, the hydrological and mechanical properties of the GBFS depends on the micro-structure of the material, while the generation of the calcium silicate hydrate can be neglected. On the other hand, for longer curing time the influence of the calcium hydrate silicate generation becomes significant. Finally, it was concluded that mixing the GBFS with sand is a simple efficient way to control the time dependent mechanical, hydrological and chemical properties of the GBFS, however, the combined effect of the hydration reaction rate and the void ratio developments in response to the mixing ratio and the curing time should be properly considered to optimize utilizing the GBFS.

1. Introduction

The Granulated Blast Furnace Slag (GBFS) is an industrial byproduct that is produced through the iron manufacturing process. During the manufacturing process, the molten slag is cooled rapidly by quenching with water resulting in a vitreous granulated byproduct called the GBFS. As reported by Nippon slag association (2016), every year about 20 million tons of GBFS are produced as a manufacturing byproduct. Since there is a continuous demand on the iron for supporting the development of nations, the continual generation of the GBFS as construction materials is expected.

Considering the Southeast Asian countries, a remarkable increase in the GBFS generation in response to the huge demand on steel production to support the

[1] Graduate student, Geotechnical Engineering Laboratory, Department of Civil Engineering, Faculty of Engineering, Kyushu University, 744 Motooka, Nishi-ku, Fukuoka 819-0395, JAPAN, tc100693@gmail.com
[2] Professor, Geotechnical Engineering Laboratory, Department of Civil Engineering, Faculty of Engineering, Kyushu University, 744 Motooka, Nishi-ku, Fukuoka 819-0395, JAPAN, yasufuku@civil.kyushu-u.ac.jp
[3] Associate professor, Geotechnical Engineering Laboratory, Department of Civil Engineering, Faculty of Engineering, Kyushu University, 744 Motooka, Nishi-ku, Fukuoka 819-0395, JAPAN, ishikura@civil.kyushu-u.ac.jp
[4] Graduate student, Geotechnical Engineering Laboratory, Department of Civil Engineering, Faculty of Engineering, Kyushu University, 744 Motooka, Nishi-ku, Fukuoka 819-0395, JAPAN, adel_owaisi@yahoo.com
Note: Discussion on this paper is open until June 2019

developing process is highly expected. On the other hand, Japan as a developed country with the infrastructure construction phase almost accomplished is expected to experience significant reduction in the demand on steel. In addition, the challenges related to the reduction of population and generation of other byproducts with the necessity to be dumped became one of the most alarming problems in Japan. Overall, finding innovative utilization methods and applications for the GBFS considering the natural variations in such material characteristics is a necessity (Sakata et al., 2014; Ismanti et al., 2017). It must be noted that the GBFS is mainly utilized in cement production accounting for 70% of the total utilized weight, while the geotechnical engineering applications accounts only for 2%.

Different GBFSs generated at different mills vary slightly in their characteristics depending on the steel mill generation process. As reported by the Japanese Geotechnical Society (2010), a light weight slag has a unit weight in the range of 9-14 kN/m^3, large angle of internal friction ($\phi \geqq 35°$), particle size similar to natural sands and high water permeability due to the high void ratio (k_s) ranging in the order of 10^{-2} to 10^{-4} m/s. In addition, it imposes the potential to develop strength as a result of the stiffening behavior directly linked to its hydration characteristics which can develop significantly with time.

Takahashi (2002) investigated the hardening process of the GBFS due to the reaction with water (hydration phenomenon). It was found that when the GBFS is in contact with water the hydration process takes place, where some ions such as calcium (Ca^{+2}), silica ($H_2SiO_4^-$), aluminate ($Al(OH)_4^-$) and other ions react with water generating many compounds including calcium silicate hydrate covering the GBFS particles and filling the inter-particle voids. A consolidation phenomenon was also reported and justified to be a result of the calcium silicate hydrate filling the inter-particle voids and squeezing the water out.

Many studies reported using the GBFS as an earthwork material such as geotechnical filler for soil embankments or as a ground improvement material. Considering the case where the GBFS is used as lightweight geotechnical filler for soil embankments, Matsuda (2012) reported that only slight reduction in the hydraulic conductivity was observed during and after the construction process. Based on that in addition to the hardening properties of the GBFS, it can be considered as a promising light weight embankment filling material for short and long term extended geotechnical construction projects.

Shinozaki (2006) investigated the applicability of using the GBFS as a ground improving material. It was confirmed that the GBFS has an internal friction angle of 35° and can be used as a major substitutive material for replacing the sand material when applying the sand compaction pile (SCP) method, which is considered as a low cost soft soil improvement technique, specially under large GBFS pile-clay replacement condition. On the other hand, when using low GBFS pile-clay replacement ratio, some problems related to the consolidation of the natural land (clayey material) was reported. This was confirmed to be a result of crushing the GBFS particles while preparing the GBFS-sand piles resulting in significantly decreasing the hydraulic conductivity of the GBFS-sand mixed piles.

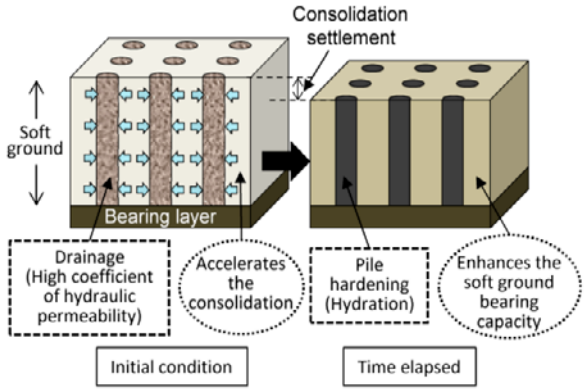

Fig. 1. Proposed ground improvement system. Utilizing the GBFS in the SCP system, where the consolidation process is accelerated as a result of the GBFS piles high hydraulic permeability. With time passing, the hydration of the GBFS piles enhances the bearing capacity of the surrounding soft ground.

Based on the former review, the GBFS can be considered as a promising construction material that has the potential to be significantly utilized in various geotechnical engineering applications. This study aims at investigating the geotechnical properties of the GBFS as a replacing material for sandy soil in SCP systems. Through this paper the time dependent mechanical and hydrological properties of the GBFS as a substitutive material are investigated. Furthermore, for the purpose of extending the effective utilization of the GBFS, the low GBFS-sand piles replacement ratio SCP construction system for soft soil improvement is also investigated. Finally, natural silica sand-GBFS mixture was proposed as a simple effective way to control and optimize the time dependent hardening and hydraulic conductivity development of the GBFS-sand piles.

2. Proposed ground improvement system

A schematic diagram showing the proposed ground improvement system utilizing the GBFS is shown in **Fig. 1**. The proposed system considers utilizing the

Table 1. Chemical composition of GBFS and ordinary Portland cement (Yamanaka et al., 1997). GBFS is highly comprised of pozzolanic material which hydrates with water and hardens with time.

Mass (%)	CaO	SiO_2	Al_2O_3	MgO	S	MnO
GBFS	42	33.6	14.9	7.3	0.9	0.2
OPC	64.2	22	5.5	1.5	0.8	-

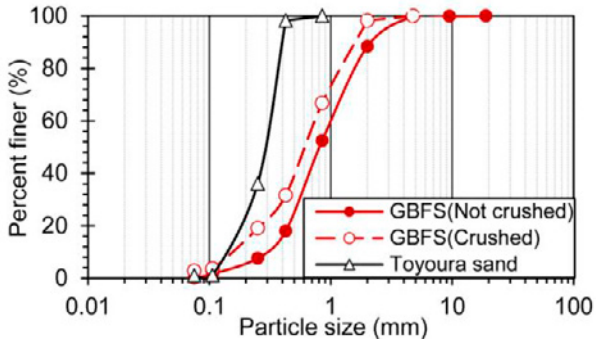

Fig. 2. Particle size distribution curve for crushed GBFS, not crushed GBFS and Toyoura sand.

Table 2. Physical properties of GBFS of the crushed GBFS, not crushed GBFS and Toyoura sand.

	ρ_s (g/cm^3)	e_{max}	e_{min}	e_0	D_{50} (mm)	U_c
GBFS (NC)	2.747	1.513	1.070	1.159	0.8	3.6
GBFS (C)	2.747	1.356	0.830	0.935	0.7	3.1
Sand	2.646	0.982	0.608	-	0.3	2.2

GBFS in the SCP method as a new soft ground improvement method for low GBFS pile-clay replacement ratio. The high permeability of the GBFS prior to complete hardening allows efficient consolidation of the surrounding soft ground. With the time passing, the GBFS gradually gains strength due to the hardening process and turns into an improved pile reinforcing the surrounding soft ground.

However, the GBFS particles experience severe particle crushing during compaction and placement of GBFS pile adopting the SCP method as reported by Takahashi (2002). This results in accelerating the hydration process and thus faster hardening rate. On the other hand, it was reported that crushing the particles significantly reduces the hydraulic conductivity of the GBFS piles.

Many researches indicated that there are various factors which significantly affect the shear strength and the hydraulic permeability of the GBFS. Accurate evaluation and control of those factors are key indices for developing an effective improvement system which will be discussed in this study. Among the affecting factors,

3. Materials and methodology

3.1 Materials

Through this study, GBFS produced at Oita works, Nippon steel and Sumitomo metal corporation, Japan 2012 was used. In addition, Toyoura standard sand which is uniformly graded silica sand was mixed with the GBFS in order to control the time dependent mechanical and hydrological properties of the GBFS piles. The chemical composition of the tested GBFS in addition to the Ordinary Portland Cement (OPC) chemical composition are shown in **Table 1** (Yamanaka et al., 1997). The particle size distribution curves in addition to the physical properties of the crushed and not crushed GBFS and Toyoura sand are shown in **Fig. 2** and **Table 2** respectively. As shown in **Fig. 2**, the GBFS falls in the range of sandy to sandy with gravel soil with similar particle size distribution ranging from (0.075 – 9.5 mm). It must be noted that the GBFS is a highly porous material with void ratio greater than 1, thus imposes high hydraulic conductivity values, where this can be attributed to the production mechanism where huge amounts of air bubbles are entrapped in the molten slag during the rapid cooling stage by quenching it with water.

In order to simulate the particle crushing of the GBFS during the construction and placement of the GBFS piles into the soft ground using the SCP ground improvement system, the GBFS particles were crushed in a systematic way conducted according to JISA 1210 (Test method for soil compaction using a rammer) compaction method. Initially the GBFS was dried in an oven for 24 hours at 110 °C. Then the oven dried GBFS was compacted into a mold with dimensions of 10 cm in diameter and 30 cm in height. GBFS was placed in the mold into 10 cm layers to assure uniform and consistent compaction energy, where each layer was compacted using a 2.5 kg rammer allowed to free fall for 30 cm before hitting the GBFS surface. The test was repeated three times to assure the accuracy and repeatability of the adopted crushing method. The method was verified by comparing the particle size distribution of the crushed sample to the particle size distribution for in situ installed GBFS-piles as reported by Shinozaki (2006), where well agreement was confirmed. As demonstrated in **Table 2**, the maximum and minimum void ratios slightly decreased after crushing the GBFS. In addition, by crushing the GBFS sample, the median diameter significantly decreased from 0.9 mm to 0.6 mm.

3.2 Samples preparation

Crushed and not crushed GBFS samples were

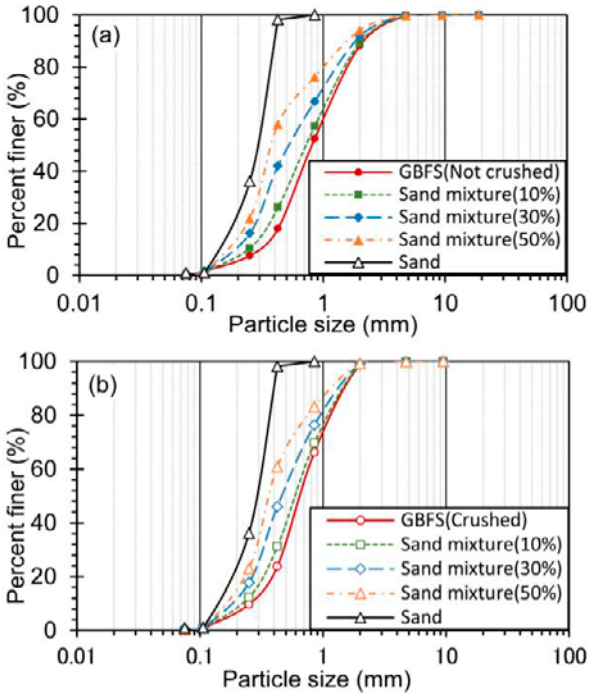

Fig. 3. Particle size distribution curves for GBFS-sand mixtures. (a) Particle size distribution curves for the not crushed GBFS-sand mixtures. (b) Particle size distribution curves for the crushed GBFS-sand mixtures. The curves were obtained by taking the weighted average of the natural sand, crushed and not crushed GBFS in relevance to the replacement ratio.

Table 3. Adopted crushed GBFS samples, not crushed GBFS samples and GBFS- sand mixtures and their physical properties.

	ρ_s (g/cm^3)	e_{max}	e_{min}	e_0	D_{50} (mm)	U_c
GBFS-NC	2.747	1.513	1.070	1.159	0.8	3.6
GBFS-NC-Sand 10%	2.621	1.332	0.865	0.959	0.8	4.0
GBFS-NC-Sand 30%	2.624	1.145	0.715	0.801	0.6	3.8
GBFS-NC-Sand 50%	2.642	1.031	0.609	0.694	0.4	2.7
GBFS-C	2.747	1.356	0.830	0.935	0.7	3.1
GBFS-C-Sand 10%	2.644	1.210	0.713	0.813	0.6	3.4
GBFS-C-Sand 30%	2.655	1.076	0.634	0.722	0.5	3.4
GBFS-C-Sand 50%	2.657	1.008	0.604	0.685	0.4	2.6
Sand	2.646	0.982	0.608	-	0.3	2.2

prepared by pouring the GBFS into a plastic mold with a diameter of 5 cm and 10 cm in height. Each layer was placed using identical placement techniques and then compacted by tamping the sides of the mold using a hammer to the desired relative density (D_r = 80%).

GBFS-sand mixed samples were prepared by systematically replacing the GBFS by sand. In total,

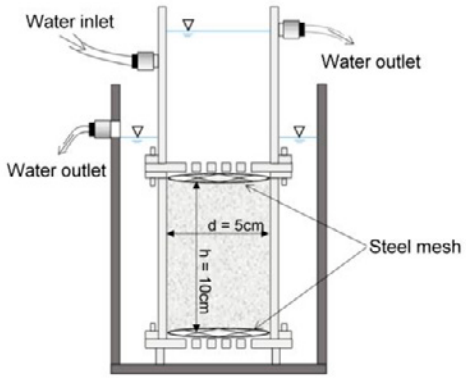

Fig. 4. Coefficient of hydraulic conductivity determination adopted testing setup. Constant water head conditions can be maintained while testing.

four different replacement ratios of 0%, 10%, 30% and 50% by weight were adopted. Initially the not crushed GBFS was mixed with sand using the assigned ratio. For crushed GBFS-sand mixed samples, the not crushed GBFS-sand mixture was then crushed using the previously mentioned crushing method in section 3.1. After preparing the crushed and not crushed GBFS-sand mixtures, the samples were compacted into the same molds and adopting the same placement techniques for GBFS samples. In general, cured and not cured samples were used for investigating the mechanical and hydrological properties of the GBFS and GBFS-sand mixed samples. Samples were cured for 7, 21, 84, 140 and 252 days for the hydrological properties tests, while 14, 21, 56, 84 days curing time was adopted for the mechanical properties tests.

The physical properties and the particle size distribution curves of the crushed and not crushed GBFS-sand mixtures are presented in **Figs. 3 (a), (b)** and **Table 3** respectively. It should be noted that the particle size distribution curves of the crushed and not crushed GBFS-sand mixtures are obtained by taking the weighted average of the natural sand, crushed and not crushed GBFS in relevance to the replacement ratio.

3.3 Experimental step and testing conditions

3.3.1 Hydrological properties

The hydrological properties were tested by determining the hydraulic permeability characteristics considering (1) the influence of crushing the GBFS particles, (2) development of water flow with time, and (3) influence of mixing the GBFS with sand. A simple experimental setup which allows for applying the constant head conditions (JIS A 1218) to determine the hydraulic conductivity of the prepared samples with a relative density of 80% (confined state) were developed in the laboratory as shown in **Fig. 4**. Measurement was carried

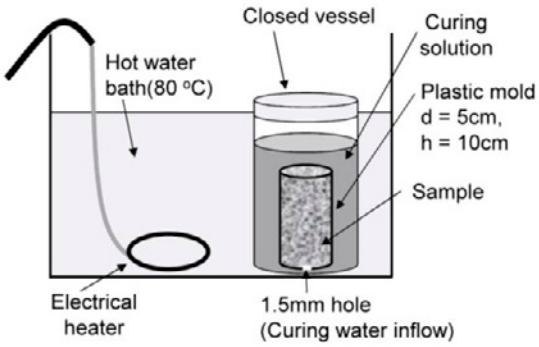

Fig. 5. Curing water bath. Curing was carried out by soaking the samples into a sodium hydroxide aqueous solution bath with a temperature of 80 °C.

Table 4. Water bath curing conditions.

	D_r (%)	GBFS-sand mixtures ratio (%)	Curing solution	Water bath temperature (°C)
GBFS (Not crushed, Crushed)	80	0, 10, 30, 50	Aqueous sodium hydroxide solution (pH≈ 12)	80

out under room temperature and pressure. Samples were placed in a dry condition into the hydraulic conductivity molds, and then constant water head was maintained through the testing period. The saturated hydraulic of conductivity was measured after 7, 21, 84, 140 and 252 days from applying the water head to the tested samples.

3.3.2 Mechanical properties

Considering the crushing of the GBFS particles and the influence of mixing the GBFS with sand, the mechanical properties of the crushed GBFS, not crushed GBFS and GBFS-sand mixtures were investigated using the static triaxial test (JGS 0524-2009) and the unconfined compression test (JIS A 1216). The shear strength characteristics were determined using the static triaxial test under the consolidated drained conditions. For this test, specimens were prepared adopting the water pluviation method by filling the membrane (attached to a mold) with water then pouring the oven dried sample and tamping the sides of the membrane with a hammer to achieve consistent and uniform densities for the prepared samples. The samples are 5 cm in diameter and 10 cm in height with a relative density of 80%. Saturation was carried out using the double negative pressure method, after that deaerated water was used to flush the occluded air bubbles in the sample. Tests were carried out under three confining pressures 50 kPa, 100 kPa and 200 kPa with back pressure maintained at 200 kPa and 0.3% strain rate.

The unconfined compression test was also used to investigate the mechanical properties of the crushed GBFS, not crushed GBFS and GBFS-sand mixtures. Cured samples were tested, where in order to accelerate the curing process, samples were soaked into a sodium hydroxide aqueous solution bath with a temperature of 80 °C. **Fig. 5** and **Table 4** demonstrate the curing setup and the curing conditions respectively. A strain rate of 1% per minute for the unconfined compression tests was adopted for all tested samples.

3.3.3 Chemical properties

It was reported (Daimon et al., 1982; Tokumitsu et al., 2000; Takahashi K et al., 2002) that when the GBFS is in contact with water the hydration process takes place generating chemical compounds initially filling the inter-particle voids adjacent to the particle contact point after that covering the GBFS particles. In order to investigate the development of the time dependent hydration process for crushed GBFS, not crushed GBFS and GBFS-sand mixtures, the selective dissolution method (Wada et al., 2015) which allows quantifying the hydration reaction by dissolving the hydrate compounds and determining its ratios was carried out.

Selective dissolution tests were carried out by oven drying the GBFS at 110 °C for 24 hours, then pouring 1.0 g of the GBFS in a compound solution comprised of acetone 70 ml, methanol 30 ml, salicylic acid 5.0 g in an Erlenmeyer flask. The sample and Erlenmeyer flask is then agitated using a magnetic stirrer with a rotation speed of 350 rpm for about 1 hour, the sample then was left for 24 hours afterwards separated by a suction filtration using a quantitative filter paper with a pore diameter of 1.0 μm. The filter paper with the obtained residue was then heated at 850 °C for one hour in order to incinerate the filter paper. The sample was moved to the desiccator and left to cool down to the room temperature, and then the mass of the residue was determined using a balance with a resolution of 0.0001 g. The hydration reaction (R) was then calculated as follows:

$$R(\%) = 100 - \frac{m_h}{m_d \times \left(1 - \frac{L_i}{100}\right)} \quad [1]$$

Where m_h is the mass of the residue after heating at 850 °C (g); m_d is the mass of GBFS after heating at 110 °C (g) and L_i is the loss of ignition (%) of the GBFS. It must be noted that the selective dissolution tests were carried out using the same samples which were tested with the unconfined compression apparatus.

4. Results and discussion

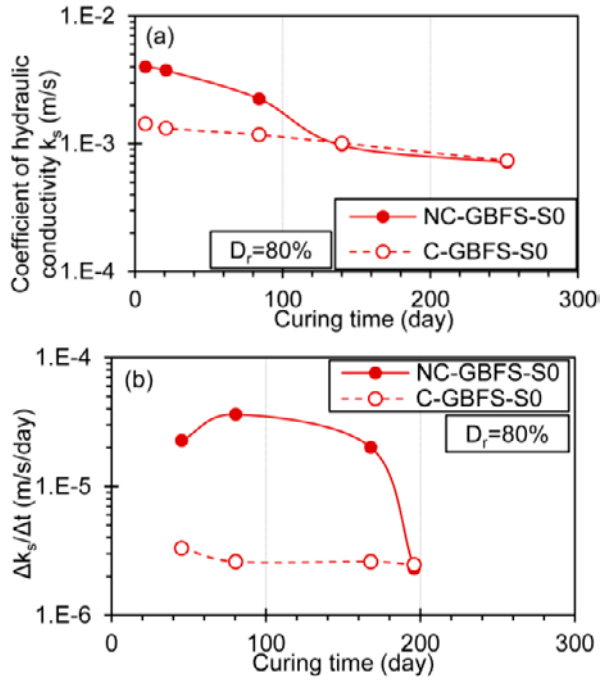

Fig. 6. Hydrological properties. (a) Development of the saturated coefficient of hydraulic conductivity with time for crushed and not crushed GBFS. (b) Reduction rate of the coefficient of hydraulic conductivity [Δk_s / Δt] for crushed and not crushed GBFS.

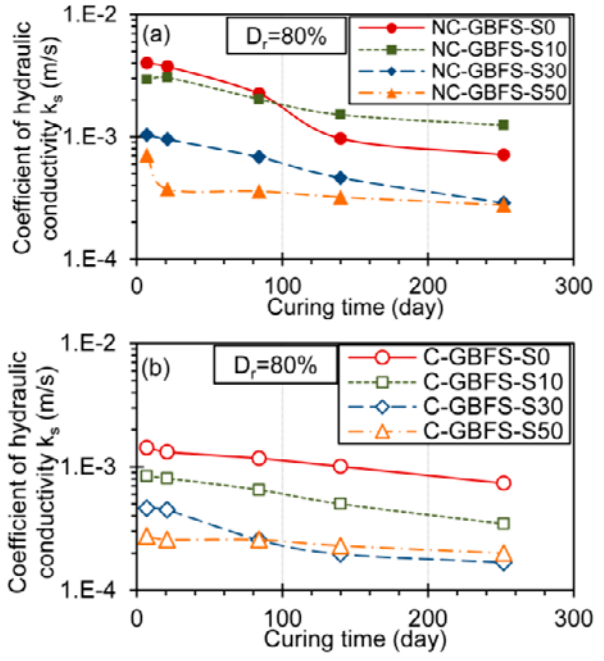

Fig. 7. GBFS-sand mixture hydrological properties. (a) Development of the saturated coefficient of hydraulic conductivity with time for not crushed GBFS- sand mixtures. (b) Development of the saturated coefficient of hydraulic conductivity with time for crushed GBFS- sand mixtures.

4.1 Hydrological properties

Constant head permeability tests were carried out for crushed GBFS, not crushed GBFS and GBFS-sand mixtures. The saturated coefficient of hydraulic conductivity was measured after 7, 21, 84, 140 and 252 days after applying the water head to the tested samples. **Figs. 6 (a)** and **(b)** show the development of the saturated coefficient of hydraulic conductivity with time and the reduction of the coefficient of hydraulic conductivity rate for crushed and not crushed GBFS respectively. It should be noted that the reduction of the coefficient of hydraulic conductivity rate was calculated by taking the average of three consecutive points and plotted against the average curing time, except for the last plot where it was averaged on the last two consecutive points. As demonstrated in **Fig. 6 (a)**, initially the saturated coefficient of hydraulic conductivity for not crushed GBFS is significantly higher than the crushed GBFS coefficient of hydraulic conductivity (at 7 days) which can be attributed to the significant difference in the initial void ratio for the crushed and not crushed GBFS samples. However, with time passing the saturated coefficient of hydraulic conductivity dramatically decreases for the not crushed GBFS, while it decreases slightly for the crushed GBFS. Where as shown in **Fig. 6 (b)**, the reduction rate increases slightly for the not crushed GBFS then decreases dramatically after 140 days, while the crushed GBFS reduction rate decreases and stables in a short time (21 days). Finally, it can be observed that starting from 140 days, the saturated coefficient of hydraulic conductivity is almost the same for both the crushed and not crushed GBFS samples with almost the same reduction rate. The reduction of the saturated hydraulic of conductivity for both the crushed and not crushed GBFS can be justified to be a result of the generation of the calcium silicate hydrate which gradually covers the GBFS particles and fills the pores thus reducing the void ratio and increasing the tortuosity of the GBFS micro-structure.

Figures 7 (a) and **(b)** show the development of the saturated coefficient of hydraulic conductivity with time for the crushed GBFS-sand mixtures and not crushed GBFS-sand mixtures respectively. As shown in **Figs. 7 (a)** and **(b)**, mixing the GBFS with sand significantly reduces the initial coefficient of hydraulic conductivity with a maximum reduction of one order when mixing with 50% with sand for both crushed and not crushed GBFS samples. In addition, it can be observed that increasing the mixing ratio has the influence of inducing a gentler reduction rate with significantly reducing the coefficient of hydraulic conductivity (up to one order) for both crushed and not crushed GBFS-sand mixtures in comparison to

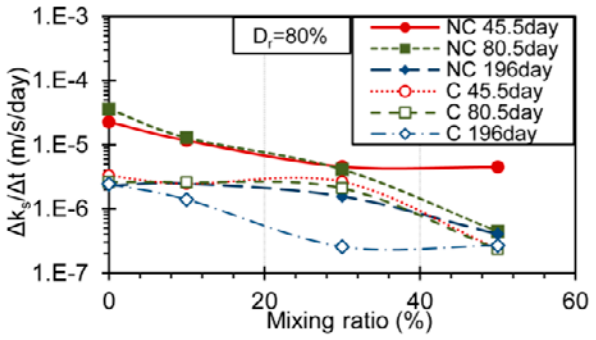

Fig. 8. Reduction rate of the coefficient of hydraulic conductivity [Δk_s / Δt] for crushed and not crushed GBFS-sand mixtures.

the not mixed samples.

Fig. 8 shows the influence of mixing GBFS with sand on the reduction of the coefficient of hydraulic conductivity rate with time for both crushed and not crushed mixtures. It can be observed that increasing the GBFS-sand mixing ratio has the influence of suppressing the reduction of the hydraulic conductivity rate. It must be noted that the reduction of the coefficient of hydraulic conductivity rate significantly decreases up to one order difference for prolonged curing times for both crushed and not crushed mixtures.

4.2 Mechanical properties

The mechanical properties of the crushed GBFS, not crushed GBFS and GBFS-sand mixtures were investigated using the static triaxial test under the consolidated drained conditions and the unconfined compression test. **Figs. 9 (a), (b)** and **10 (a), (b)** show the stress ratio (η = q/p`) versus the axial strain and the relation between the volumetric strain and the axial strain for both the not crushed GBFS and the crashed GBFS samples respectively. The deviatoric stress q and the effective stress p` were calculated as follows:

$$q = \sigma_1 - \sigma_3 \qquad [2]$$

$$p' = \frac{\left(\sigma'_1 + 2\sigma'_3\right)}{3} \qquad [3]$$

Where σ_1 is the maximum principal stress; σ_3 is the minimum principal stress; σ'_1 is the effective maximum principal stress and σ'_3 is the effective minimum principal stress.

As illustrated in **Figs. 9 (a)** and **10 (a)**, the ultimate stress ratio decreases by increasing the confining pressure for both crushed and not crushed GBFS samples. Considering the not crushed GBFS samples, the ultimate stress ratio was achieved at axial strain values higher than 5%. On the other hand, considering

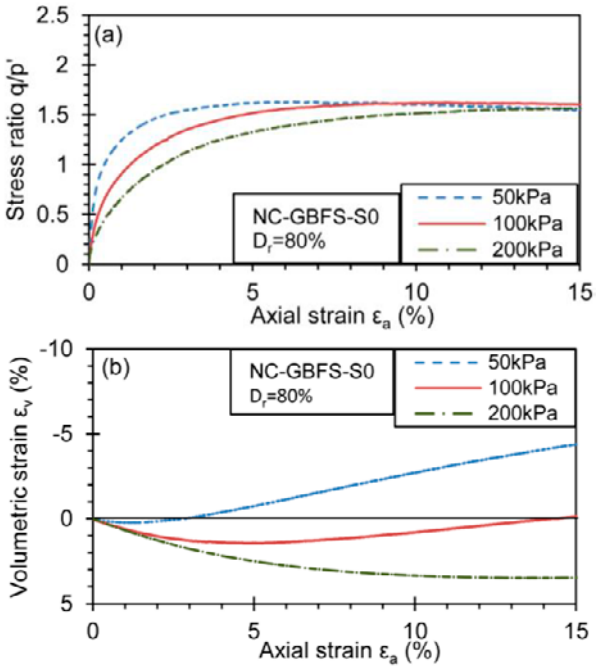

Fig. 9. Not crushed GBFS mechanical properties [triaxial tests]. (a) Stress ratio (η = q/p`) versus axial strain under 50, 100 and 200 kPa confining pressure. (b) Volumetric strain versus axial strain under 50, 100 and 200 kPa confining pressure.

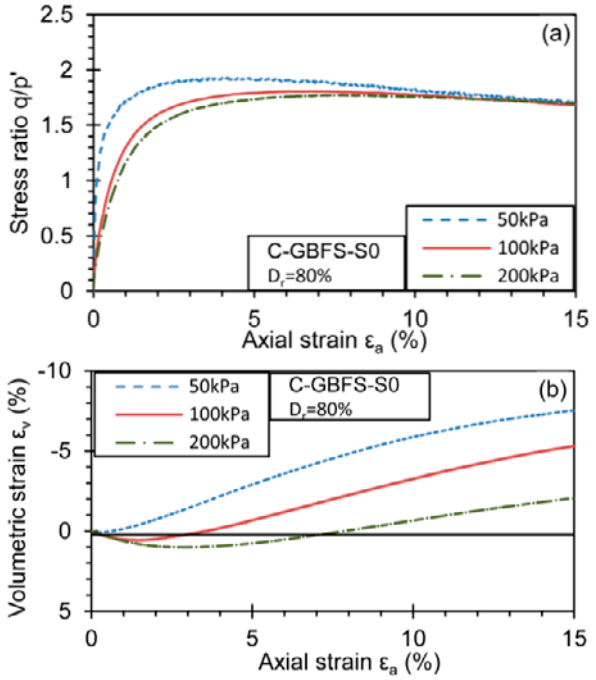

Fig. 10. Crushed GBFS mechanical properties [triaxial tests]. (a) Stress ratio (η = q/p`) versus axial strain under 50, 100 and 200 kPa confining pressure. (b) Volumetric strain versus axial strain under 50, 100 and 200 kPa confining pressure.

the crushed GBFS samples, the ultimate stress ratio was achieved at axial strain values less than 5%, where this can be attributed to the small initial void ratio (e_o) which is translated into higher density for the same material

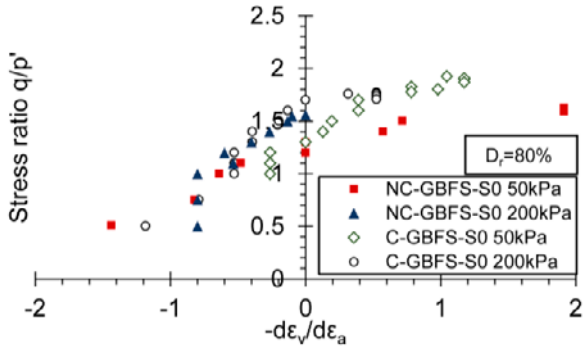

Fig. 11. Dilatancy of Crushed and not crushed GBFS. The Stress ratio versus volumetric to axial strain ratio [–$d\varepsilon_v$/ $d\varepsilon_a$] under 50 and 200 kPa confining pressure for crushed and not crushed GBFS is illustrated.

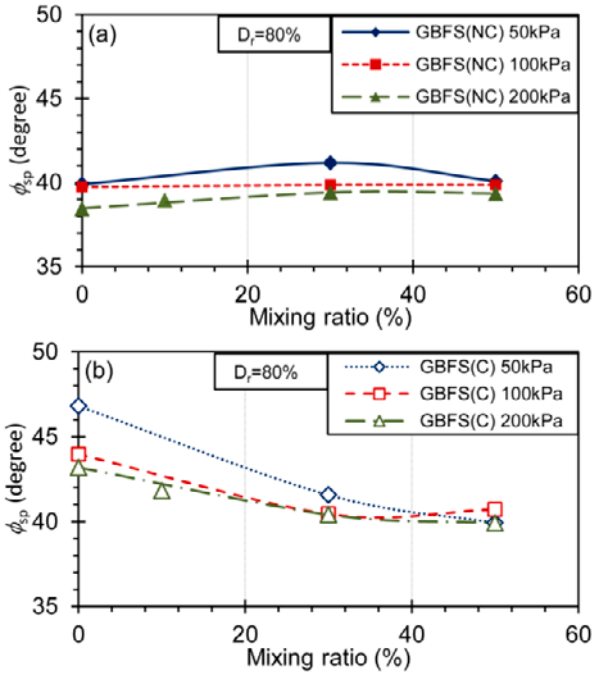

Fig. 12. GBFS-sand mixing ratio influence on the internal friction angle development under low, moderate and high confining pressure (σ_r). (a) Not crushed-sand mixtures. (b) Crushed-sand mixtures.

(GBFS).

Comparing the stress ratio for crushed GBFS to the stress ratio of the not crushed GBFS samples under various confining pressure values, it can be observed that the crushed GBFS imposes higher stress ratio within the range of (0– 15%) axial strain range, however, for axial strain values larger than 15%, the stress ratios for both crushed and not crushed GBFS samples emerge almost to the same value.

As depicted in **Figs. 9 (b)** and **10 (b)**, the volumetric strain exhibits an expansion tendency when the confining pressure is small for both crushed and not crushed GBFS samples, while it exhibits a contraction tendency for high confining pressure values. The contraction tendency for both crushed and not crushed GBFS samples can be attributed to the crushing of the slag particles under high confining pressure values. However, it must be noted that the degree of contraction is significantly larger for not crushed samples compared to the crushed sample as a result of the differences in angularity and micro-structure of the crushed and not crushed GBFS particles.

Figure 11 shows the stress ratio versus volumetric to axial strain ratio [–$d\varepsilon_v$/ $d\varepsilon_a$] for the crushed and notcrushed GBFS under 50 kPa and 200 kPa confining pressure. It can be observed that the crushed and not crushed GBFS samples show similar dilatancy characteristics under various confining pressure values [low and high].

Figures 12 (a) and **(b)** illustrate the relationship between the GBFS-sand mixing ratio and the internal friction angle (ϕ_{sp}) under low, moderate and high confining pressure (σ_r) for not crushed GBFS-sand and crushed GBFS-sand mixtures respectively. The internal friction angle ϕ_{sp} was calculated as follows:

$$\frac{q}{p'} = \frac{6\sin\phi_{sp}}{\left(3-\sin\phi_{sp}\right)} \quad [4]$$

$$\sin\phi_{sp} = \frac{3\left(\frac{q}{p'}\right)}{\left(\frac{q}{p'}+6\right)} \quad [5]$$

Where q/p' is the stress ratio. As depicted in **Figs. 12 (a)** and **(b)**, it can be observed that for zero mixing ratio, the crushed GBFS imposes higher internal friction angle compared to the not crushed GBFS. Mixing the crushed GBFS with sand results in decreasing the internal friction angle. On the other hand, mixing the not crushed GBFS with sand has very slight influence on the internal friction angle that can be neglected. It must be noted that mixing the crushed GBFS with high sand ratios (> 30%) results in decreasing the internal friction angle till reaching almost the same value of the not crushed GBFS and the not crushed GBFS-sand mixtures internal angle of friction which is about 40°.

Figure 13 demonstrates the unconfined compressive strength development of the not crushed GBFS, crushed GBFS samples versus the curing time. It must be noted that specimens with unconfined compressive strength of 0 (kN/m^2) indicate very low compressive strength due to the insufficient curing time and therefore not self-supporting samples where it could not be tested. Comparing the crushed GBFS to the not crushed GBFS samples, it can be observed that the unconfined compressive strength of the crushed samples is significantly larger than the not crushed samples compressive strength, where for curing time exceeding

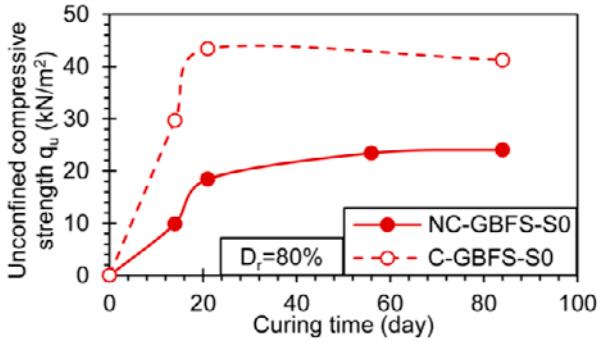

Fig. 13. Unconfined compressive strength of the crushed and not crushed GBFS development with time.

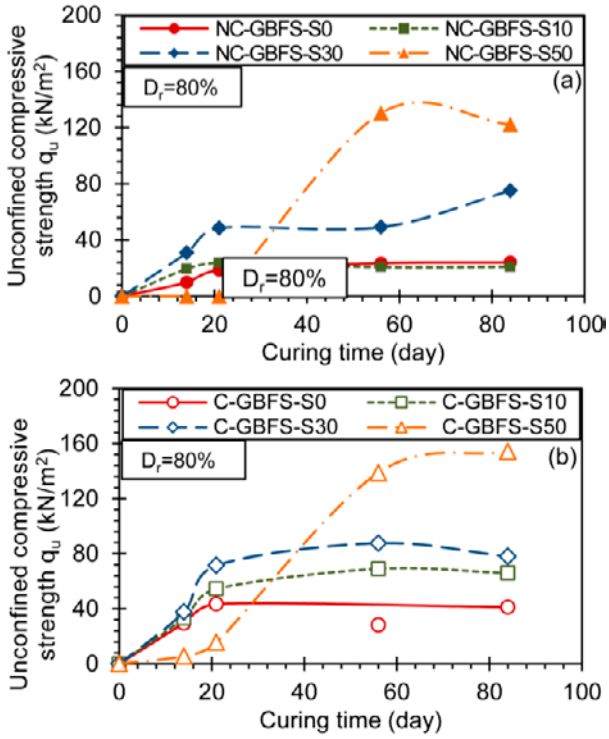

Fig. 14. Unconfined compressive strength of GBFS-sand mixtures. (a) Not crushed GBFS-sand mixtures (b) Crushed GBFS-sand mixtures.

20 days, crushed GBFS samples impose almost as twice as the unconfined compressive strength of the not crushed GBFS samples. This might be attributed to the micro-structure of the GBFS particles, where the crushing results in increasing both the number of contact points between particles and the surface area which enhances the chemical reaction and accelerates the GBFS hardening process.

As illustrated in **Figs. 14 (a)** and **14 (b)**, it can be concluded that mixing the crushed GBFS or the not crushed GBFS with sand significantly enhances the compressive strength. Where increasing the mixing ratio results in strengthening the sample, this can be related to the fact that the initial void ratio becomes smaller by filling

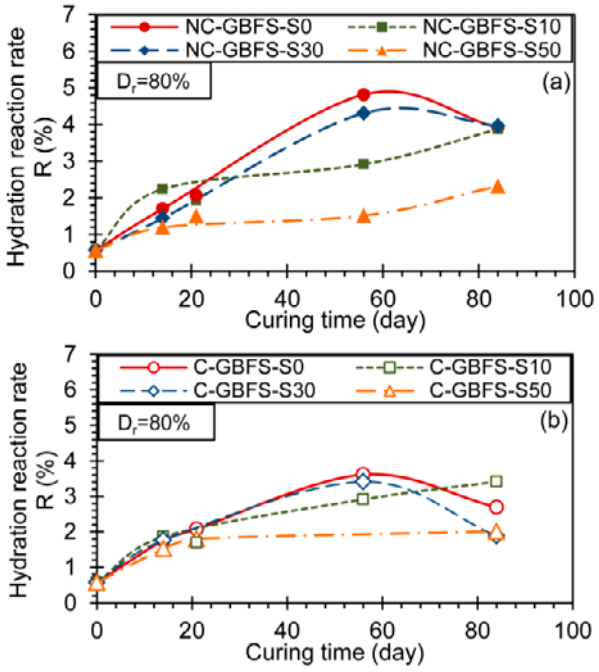

Fig. 15. The time dependent hydration reaction rate development. (a) Not crushed-sand mixtures. (b) Crushed-sand mixtures.

the pores with sand. It must be noted that the compressive strength development rate for 50% GBFS-sand mixture is significantly lower than the other ratios due to the low GBFS percentage comprising the sample and thus results in lower hardening rate, however with time passing the combined effect of reducing the void ratio by filling the pores with sand and the slow hardening results in the highest compressive strength values in comparison to the lower mixing ratios.

4.3 Chemical properties

Figures 15(a) and **15(b)** show the time dependent hydration reaction rate development for the not crushed GBFS, crushed GBFS and GBFS-sand mixtures. As indicated by the solid lines through **Figs. 15(a)** and **15(b)** representing the not crushed and crushed GBFS samples, it can be observed that the hydration reaction rate is slightly higher for crushed GBFS samples in comparison to the not crushed GBFS samples with the difference growing bigger with time. This trend can be attributed to the difference in the total surface area between the crushed and not crushed GBFS samples.

For both crushed and not crushed GBFS, mixing with sand has the influence of decreasing the hydration reaction rate (R), where the percentage of GBFS decreases by increasing the mixing ratio thus leads to less total hydration surface and finally less amount of hydrate silicate to be generated. It must be noted that increasing the mixing ratio induces reduction in the

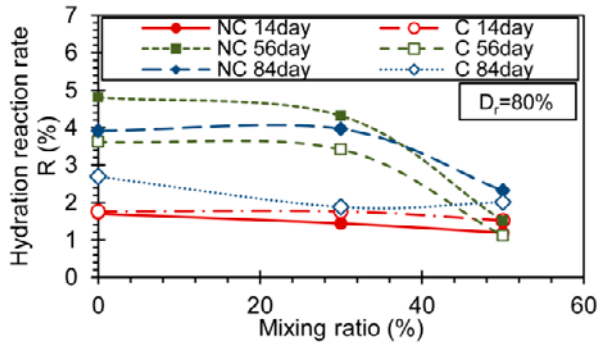

Fig. 16. The influence of mixing the crushed and not crushed GBFS with natural silica sand on the hydration reaction rate after 14, 56 and 84 curing days.

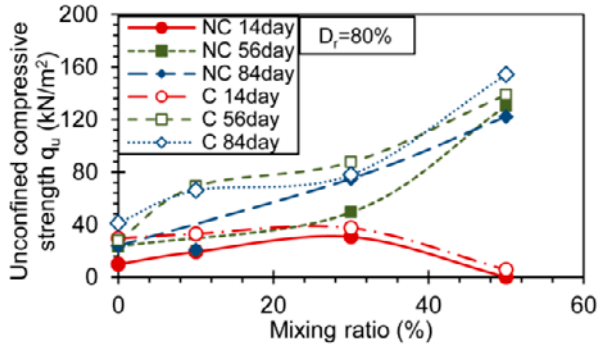

Fig. 17. The influence of mixing the crushed and not crushed GBFS with natural silica sand on the unconfined compressive strength after 14, 56 and 84 curing days.

generation of the hydrate silicate rate due to the reduction in the GBFS total surface area. Finally it can be concluded that mixing the GBFS with sand is a simple efficient way of suppressing the hydrate silicate generation rate, which directly affects the hydrological and mechanical properties of the proposed SCP system.

Figures 16 and **17** show the influence of mixing GBFS with sand on the hydration reaction rate and on the unconfined compressive development with time respectively. It can be observed that for early curing stages (14 days), the crushed GBFS samples and mixtures impose higher hydration reaction rate and higher unconfined compressive strength in comparison to the not crushed GBFS samples and mixtures. At this early stage, the compressive strength of those samples and mixtures is a function of the void ratio, where the hydration reaction influence is minor and thus can be neglected. As the curing time increases, the hydration reaction significantly increases. For curing periods exceeding (14 days), the not crushed samples and mixtures impose higher hydration reaction rate in comparison to the crushed GBFS samples and mixtures. On the other hand, the crushed GBFS samples and mixtures exhibit higher unconfined compressive strength compared to the not crushed GBFS samples and mixtures. This can be attributed to the growing influence of the hydrate silicate generation as the hydration process proceeds. At early stages, mixing the crushed or the not crushed GBFS with sand has slight influence on the hydration reaction rate and on the unconfined compressive strength. However, with the curing time passing, the addition of sand influence becomes more significant. Where at those stages of curing, the GBFS samples and mixtures unconfined compressive strength is function of the combined effect of the hydration reaction rate and the void ratio development. Finally, it can be concluded that in order to efficiently utilize the proposed system, the combined effect of the hydration reaction rate development and the void ratio development in response to the mixing ratio and the curing time should be properly considered to optimize utilizing the GBFS-sand piles in the SCP system.

5. Conclusions

The curing time and the crushing effect on the utilization of the granulated blast furnace slag in the soil compaction piles system were investigated. The development of the hydrological, mechanical and chemical properties of the utilized GBFS was investigated. In addition, silica sand was used as an additive material to control the development of the utilized GBFS properties.

It was found that for early hydration stage, the hydrological and mechanical properties of the GBFS depends mainly on the micro-structure of the material which can be characterized by the initial void ratio, while the generation of the calcium silicate hydrate (hydration process) influence is not significant and can be neglected. Through this stage, the not crushed GBFS imposes higher hydraulic conductivity, lower stress ratio and lower unconfined compressive strength in comparison to the crushed GBFS.

On the other hand, for longer curing time, the not crushed GBFS samples impose higher hydration reaction rate in comparison to the crushed GBFS samples. The not crushed samples exhibited significant reduction in the hydraulic conductivity, while slight stable reduction was observed for the crushed GBFS samples. It must be noted that after allowing prolonged hydration, the hydraulic conductivity of the not crushed GBFS emerged to the same order as the crushed GBFS. Crushed GBFS samples exhibited higher ultimate stress ratio for axial strain values less than 15% then emerged to the same value of the not crushed GBFS. The unconfined compressive strength and the internal friction angle were higher for the crushed GBFS in comparison to the not

crushed GBFS samples due to the growing influence of the calcium hydrate silicate generation as the hydration process proceeds.

At early stages, mixing the crushed or the not crushed GBFS with silica sand has slight influence on the hydrological, mechanical and chemical properties. However, with the curing time passing, the addition of sand influence becomes more significant. It was found that mixing the GBFS with high silica sand ratio (> 30%) conceal the effect of crushing the GBFS particles on the mechanical properties and significantly suppresses the hydrate calcium silicate generation rate. It can be said that at late curing stages, the GBFS samples and mixtures unconfined compressive strength is function of the combined effect of the hydration reaction rate and the void ratio development. Finally, it can be concluded that the combined effect of the hydration reaction rate development and the void ratio development in response to the mixing ratio and the curing time should be properly considered to optimize utilizing the GBFS-sand piles in the soil compaction piles system.

Acknowledgements

The authors express their gratitude to the laboratory technical assistant Mr. Michio Nakashima for their great support.

References

Coastal development institute of technology, Nippon slag association, 1989. Manual of the granulated blast furnace slag for port and harbor construction.

Coastal development institute of technology, 2007. Technical manual of the granulated blast furnace slag for harbor and airport.

Daimon, D., Song C.T., Nishita, A., Yamaguchi, O., Kim, C.E., Tani, N., 1982. Change in the Liquid Concentration during the Hydration of Granulated Blast Furnace Slag. Gypsum & Lime, 1982(176): 3-8.

Japan geotechnical engineering, 2010. Research committee report on promotion of geotechnical utilization of the granulated blast furnace slag.

Ismanti, S., Yasufuku, N., 2017. Effect of bamboo leaf ash addition in cemented bamboo chips-sand soil mixture. Lowland Technology International, **19** (1): 13-26.

Japanese geotechnical society, 2009. Method for consolidated-drained triaxial compression test on soils. JGS 0524-2009.

Japanese Standards Association, 2009a. Methods for unconfined compression test of soils. JIS A 1216, in Japanese.

Japanese Standards Association, 2009b. Test methods for permeability of saturated soils. JIS A 1218, in Japanese.

Japanese Standards Association, 1990. Test method for soil compaction using a rammer. JIS A 1210, in Japanese.

Matsuda, H., Ishikura, R., Wada, M., Kitayamal, N., Beak, W., Tani, N., 2012. Aging effect on the physical and mechanical properties of granulated blast furnace slag as lightweight banking. Japanese Geotechnical Journal, The Japanese Geotechnical Society, **7** (1): 339-349.

Nippon slag association, 2009. Technical documentation as earthwork material.

Nippon slag association, 2015. Environmental Resources Iron and Steel Slag.

Nippon slag association, 2016. Amounts of blast furnace slag produced and used in FY 2016, Nippon slag association.

Sakata, T., Miyata, S., Satou, K., Fujikawa, T., Koga, C., 2014. Effects of initial water content and degree of compaction on shear characteristics of incineration bottom ash from disaster waste. Proceedings of 49nd Japan national conference on geotechnical engineering: 521-522.

Shinozaki, H., Matsuda, H., Sakai, E., Ono, K., Suzuki, M., Nakagawa, M., 2006. Hardening property of granulated blast furnace slag and its application to soil improvement. Journal of Japan Society of Civil Engineers C, **62** (4): 858-869.

Takahashi, K., Kikuchi, Y., Motoki, T., Suzuki, M., Nakagawa, M., 2002. Effect of hardening of granulated blast furnace slag (Part1: Effect of particle size). Abstracts of Japan society of civil engineers 57th Annual meeting: 63-64.

Takahashi, K., Kikuchi, Y., Yashima, K., Hoshi, H., Shinozaki, H., 2002. Effect of hardening of granulated blast furnace slag (Part1: Effect of various factors). Abstracts of Japan society of civil engineers 57th Annual meeting: 61-62.

Tokumitsu, N., Ishii, M., 2000. Hydration of granulated blast-furnace slag, Research reports of national institute of technology, akita college, 35: 71-75.

Wada, M., Matsuda, H., Hara, H., Igawa, N., Nakamura, S., 2015. Fundamental Study on Self-Restoration Characteristics of Granulated Blast Furnace Slag Focusing on a Hydration Reaction. Journal of the Society of the Materials Science japan, **64** (7), No.7: 573-578

Yamanaka,R., Tohyama, S., Toshikawa, Y., 1997. Utilization history of blast furnace slag and steel-making slag, Environmental technology. Kobe steel engineering reports, 47(3).

Symbols and abbreviations

ϕ	Internal friction angle
k_s	Coefficient of hydraulic conductivity
ρ_s	Soil dry density
e_{max}	Maximum void ratio
e_{min}	Minimum void ratio
e_0	Initial void ratio
D_{50}	Median diameter
U_c	Uniformity coefficient
d	Diameter
h	Height
D_r	Relative density
m_h	Mass of the residue after heating at 850 °C
m_d	Mass of GBFS after heating at 110 °C
L_i	Loss of ignition
Δk_s	Coefficient of hydraulic conductivity difference
Δt	Time difference
q	Deviatoric stress
p`	Effective stress
η	Stress ratio
σ_1	Maximum principal stress
σ_3	Minimum principal stress
σ'_1	Effective maximum principal stress
σ'_3	Effective minimum principal stress
ε_a	Axial strain
ε_v	Volumetric strain
ϕ_{sp}	Internal friction angle
σ_r	Confining pressure
$-d\varepsilon_v/d\varepsilon_a$	Dilatancy rate
q_u	Unconfined compressive strength